



## On the Effect of Source Parameters in the Predictions of Small Scale Anisotropies for UHECR Experiments

DANIEL DE MARCO<sup>1</sup>, PASQUALE BLASI<sup>2</sup>, PAOLO LIPARI<sup>3</sup>, ANGELA V. OLINTO<sup>4</sup>

<sup>1</sup> *Bartol Research Institute, University of Delaware, Newark, DE 19716, USA*

<sup>2</sup> *INAF/Osservatorio Astrofisico di Arcetri, Largo E. Fermi 5, 50125 Firenze, ITALY*

<sup>3</sup> *INFN and Dipartimento di Fisica, Università di Roma I, P. A. Moro 2, 00185 Roma, ITALY*

<sup>4</sup> *Laboratoire Astroparticule et Cosmologie (APC), Université Paris 7/CNRS, 10 rue A. Domon et L. Duquet, 75205 Paris Cedex 13, FRANCE & The University of Chicago, 5640 S. Ellis, Chicago, IL 60637, USA*  
*ddm@bartol.udel.edu*

**Abstract:** We discuss the small scale anisotropy signal predicted for present and future UHECR experiments such as Auger, Telescope Array, Auger North and EUSO. We relax the commonly used assumption that the sources are all equal and we concentrate our attention on how the expected signal depends on possible distributions of the properties of the sources such as a luminosity function or a varying maximum energy.

### Introduction

Since the first observation of a small scale anisotropy signal by the AGASA collaboration [1] there have been several attempts to use it in order to obtain information about the sources of UHECRs. In particular, if confirmed (see [2] for a discussion of its significance), this signal points toward the sources of UHECRs being astrophysical sources with a density of the order of  $10^{-5} \text{ Mpc}^{-3}$  [3, 4]. In Ref. [3] this result was obtained comparing the clustering signal expected from discrete distributions of sources with the measured one. In those simulations, as in the others, the sources are all assumed to be identical: all with the same luminosity and maximum energy. In the present paper we relax this assumption and we investigate the effects that possible distributions of the properties of the sources have on the measurable signals at the detectors. In particular we concentrate on the expected spectrum and small scale clustering signals.

### Adding a luminosity function

We assume discrete distributions of sources with density  $\rho = 10^{-\eta} \text{ Mpc}^{-3}$  and we assume that the

sources have a luminosity distribution  $dn/dL \propto L^{-\alpha}$  between  $L_{\min}$  and  $L_{\max}$ . We fix the ratio  $L_{\max}/L_{\min}$  to  $10^5$ , whereas the absolute value of  $L_{\min}$  depends on  $\alpha$  and is obtained requiring that the overall emissivity fits the one obtained from the data ( $\text{few} \times 10^{44} \text{ erg yr}^{-1} \text{ Mpc}^{-3}$  for  $E > 10^{19} \text{ eV}$ ). We consider scenarios with  $\eta = 4, 5, 6$  and  $\alpha = 0, 1, 2, 5, 10$ . In the beginning of each simulation we randomly choose the position and luminosity of each source and we assign to each source a probability of emitting protons. We then inject protons from this distribution of sources until the number of required particles arrives at the detector. We average our results over 100 realizations of the source distribution and particle propagation. For the simulation of the propagation we use the code described in [5, 3] and we assume an experiment with uniform exposure of the sky, energy resolution of 20%, angular resolution of  $1^\circ$  and an exposure of about  $10^5 \text{ km}^2 \text{ yr sr}$ . These are the typical numbers of the new generation of experiments that are now being built or designed such as: Auger, Telescope Array and Auger North. The above numbers correspond to an expected number of events above  $4 \times 10^{19} \text{ eV}$  ( $10^{20} \text{ eV}$ ) of about 1800 (75). We choose as minimum energy  $4 \times 10^{19} \text{ eV}$  and we assume that all particles are

protons and that the effects of magnetic fields can be safely neglected [3]. In order to estimate the effects that the assumed distributions have on the small scale anisotropies signal we calculate the two point correlation function of the arrival directions and we compare it with the expected one in the case of continuous sources and of discrete sources with a fixed luminosity, i.e.  $dn/dL \propto \delta(L - L_0)$ . For the two point correlation function we use a bin size of  $1^\circ$ , corresponding to the angular resolution of the experiment.

We plot the resulting two point correlation functions of simulated events above  $4 \times 10^{19}$  eV in the upper panel of Fig. 1. The black points correspond to the case of continuous sources, i.e. all points in space have the same probability of producing a particle. For each bin there are three series of colored points: green, blue and red; the colors correspond to different source densities:  $\eta = 4, 5, 6$  respectively. Each series is composed of 6 points corresponding to different luminosity distributions: the circle corresponds to fixed luminosity, the square, triangle, rhomb, cross and star correspond respectively to  $\alpha = 0, 1, 2, 5, 10$ .

Including a luminosity distribution obviously increases the chances of clustering since it basically increases the luminosity of a selected number of sources. This is visible in the plots, where the clustering is increased by a factor between 10 and 100 in some cases. The cases with the largest increase are the ones for  $\alpha = 1$  and 2 while for  $\alpha = 5, 10$  the effect has disappeared because the distribution is so steep that, in the limited number of sources contributing to the flux, the probability of finding sources with very large luminosities is quite small.

Calculating the two point correlation functions of the events above  $10^{20}$  eV, lower panel of Fig. 1, produces similar results, but in this case the spread of the points is smaller, with the maximum increase in the correlation being less than a factor 10.

Another point worth noticing is that, in the cases with the biggest increase, the error-bars are larger as one would expect with increased statistical fluctuations.

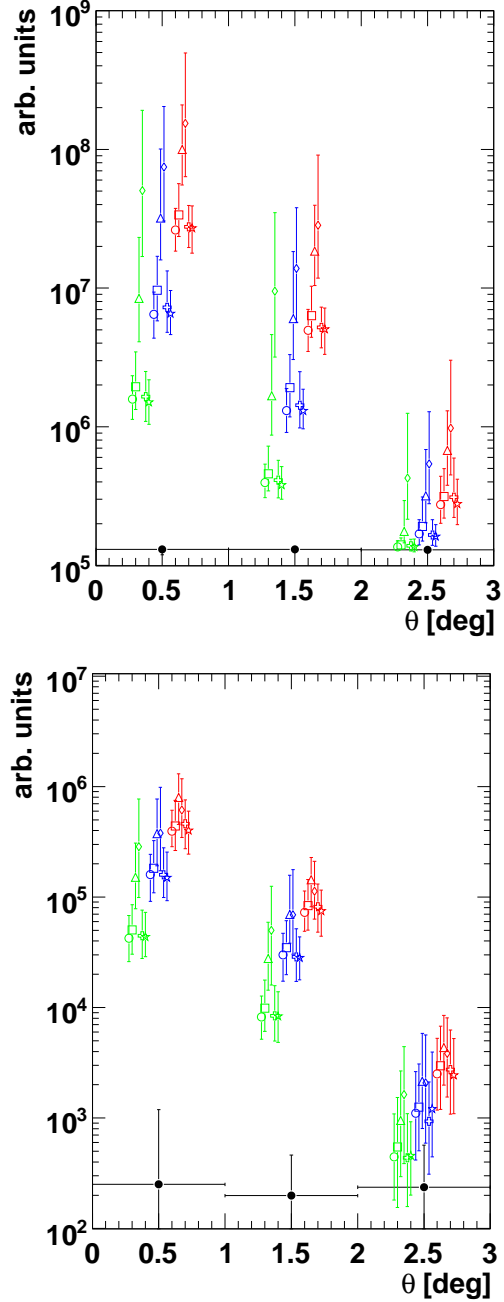


Figure 1: Two point correlation function of simulated events above  $4 \times 10^{19}$  eV (upper plot) and  $10^{20}$  eV (lower plot) for sources with different densities, different luminosity distribution functions and fixed maximum energy. See text for detailed legends.

## Adding a maximum energy distribution

In this section we relax another common assumption: we no longer require all sources to have the same maximum energy, but we assume the maximum energy to depend on the source luminosity as:  $E_{\max}(L) = E_{\max}(L_{\min})(L/L_{\min})^{\beta}$ . As it was shown in [6, 7], using this recipe and choosing appropriately  $\alpha$  and  $\beta$  one can produce, with sources injecting an  $E^{-2.1}$  spectrum, a steeper spectrum,  $E^{-(2.6-2.7)}$ , as preferred in dip transition models [8, 7]. We use  $\alpha = 2.5$ ,  $\beta = 1$ ,  $E_{\max}(L_{\min}) = 10^{17}$  eV and  $L_{\max}/L_{\min} = 10^{4.5}$  so that  $E_{\max}(L_{\max}) = 10^{21.5}$  eV. We plot our results for the two point correlation function (above  $4 \times 10^{19}$  eV) in Fig. 2.

In the plot there are three colored series of points for each bin: green, blue and red; they correspond to different densities and respectively to  $\eta = 4, 5, 6$ . In each colored set the squares correspond to discrete sources with fixed luminosity and maximum energy, the circles to discrete sources with a luminosity distribution with  $\alpha = 2.5$  and fixed maximum energy, whereas the triangles to discrete sources with luminosity and maximum energy distribution:  $\alpha = 2.5$ ,  $\beta = 1$ . The black points correspond to continuous sources. In all cases the injection is  $E^{-2.6}$ , except for the triangles for which it is  $E^{-2.1}$ . As we saw in the previous section, introducing the luminosity distribution produces a drastic effect on the two point correlation function, but adding on top of it the maximum energy distribution does not change much the result.

We plot the energy spectrum in Fig. 3, the points and colors are the same as in the previous one. The spectrum does not depend much on the luminosity distribution chosen: the points for constant luminosity (colored squares) and the ones for luminosity distribution with  $\alpha = 2.5$  (colored circles) are on top of each other. However, the spectrum shows some small effects above  $10^{20}$  eV when including the distribution of maximum energies (colored triangles). This reduction is due to statistical fluctuations in the distance to the closest source and can be understood as follows. A reduction in the flux above  $10^{20}$  eV with respect to the continuous case is already present for the three cases with discrete sources and fixed luminosity [5]. This reduction is due to the distance to the closest source

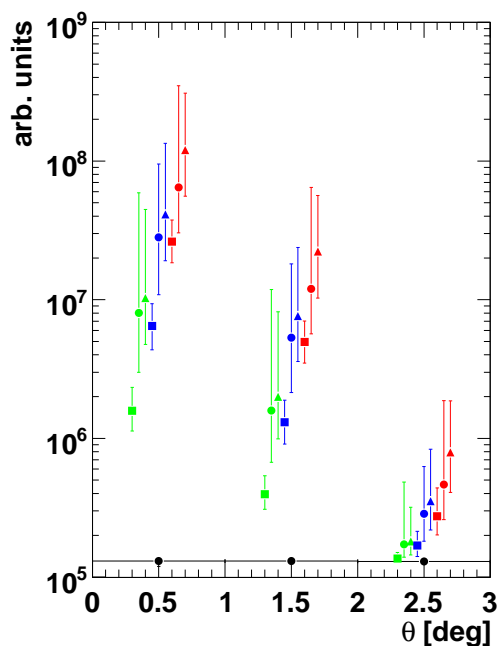


Figure 2: Two point correlation function of simulated events above  $4 \times 10^{19}$  eV for sources with different densities, different luminosity distribution functions and different maximum energy. See text for detailed legends.

that in the simulation was constrained to be larger than  $1/2\sqrt[3]{\rho}$ , the distance within which one expects on average less than one source for the given density. Including the maximum energy distribution the distance to the closest source able to produce particles above  $10^{20}$  eV is increased. Indeed, in this scenario only sources with  $L \geq 10^3 L_{\min}$  are able to produce particles with  $E \geq 10^{20}$  eV and the density of such sources is smaller, being:  $\rho' = \rho \int_{10^3 L_{\min}}^{L_{\max}} p(L) dL / \int_{L_{\min}}^{L_{\max}} p(L) dL$ .

## Conclusions

In previous attempts to investigate the clustering signal observed by AGASA the usual assumptions have been a uniform distribution of equal sources: all with the same luminosity and maximum energy. In this paper we relaxed these assumptions and we investigated the effects that this produces on the expected small scale clustering signal and on our ability to infer the important source param-

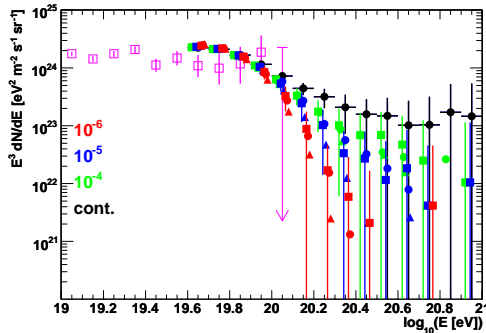


Figure 3: Energy spectra (multiplied by  $E^3$ ) expected in various scenarios. See text for detailed legends. The hollow squares with error bars represent the Auger ICRC05 data [9].

eters such as the density, luminosity and maximum energy.

First of all we showed that the inclusion of the luminosity and maximum energy distributions does not hinder the ability of future experiments to distinguish between a continuous and a discrete distribution of sources. Indeed, in all discrete cases we considered, the departure of the two point correlation function from that expected from a continuous distribution of sources is detectable at the level of tens of sigmas. On the other hand, the ability to discriminate between different densities, and thus of determining the luminosity of the sources, is greatly reduced because the inclusion of the luminosity distribution increases dramatically the spread of the two point correlation function for a given density and different luminosity distributions. Indeed, introducing a luminosity distribution function has the same effect as reducing the number of sources contributing to the flux, mimicking the effects of a smaller source density. This enhancement of the clustering is more pronounced for larger densities because the larger number of sources allows the full dynamic range of the luminosity distribution function to be probed, whereas with a smaller density the number of sources is smaller and so is the probability of having high luminosity sources. The inclusion of a distribution for the maximum energies has a less drastic effect: it does not change very much the two point correlation function, but it slightly decreases the flux of particles above  $10^{20}$  eV.

In the present paper we used the two point correlation function as an indicator of the level of small scale anisotropy expected in the various models. This is the simplest measure of small scale anisotropy you can construct, and it is very good at distinguishing between a continuous and a discrete distribution of sources, but it is not necessarily the best one to measure their density. For example it does not distinguish between a distribution with a lot of small multiplets and one with a few big ones. A better candidate for this kind of task may for example be the distribution of multiplets. Such an analysis, given sufficient statistics, can in principle allow to extract the complete luminosity function. We are working on a comparison between these approaches.

## Acknowledgments

The work of D.D.M. is funded in part by NASA APT grant NNG04GK86G. The work of P.B. is partially funded through grant PRIN-2004.

## References

- [1] N. Hayashida *et al.*, *Astrophys. J.* **522** (1999) 225
- [2] C.B. Finley and S. Westerhoff, *Astropart. Phys.* **21** (2004) 359; C.B. Finley and S. Westerhoff (HiRes Collab.), *Proc. of ICRC 2003*, Tsukuba, Japan
- [3] P. Blasi and D. De Marco, *Astropart. Phys.* **20** (2004) 559
- [4] H. Yoshiguchi *et al.*, *Astrophys. J.* **614** (2004) 43; M. Kachelriess and D. Semikoz, *Astropart. Phys.* **23** (2005) 486
- [5] D. De Marco, P. Blasi and A.V. Olinto, *Astropart. Phys.* **20** (2003) 53; *JCAP* **01** (2006) 002; *JCAP* **07** (2006) 015
- [6] M. Kachelriess and D. V. Semikoz, *Phys. Lett. B* **634** (2006) 143
- [7] R. Aloisio *et al.*, *Astropart. Phys.* **27** (2007) 76
- [8] V. Berezhinsky *et al.*, *Phys.Lett.* **B612** (2005) 147
- [9] P. Sommers *et al.* (Auger Collaboration), *Proc. of ICRC 2005*, Pune, India, *astro-ph/0507150*